


 Cite this: *Lab Chip*, 2016, 16, 2775

## Oscillatory multiphase flow strategy for chemistry and biology

Milad Abolhasani and Klavs F. Jensen\*

Continuous multiphase flow strategies are commonly employed for high-throughput parameter screening of physical, chemical, and biological processes as well as continuous preparation of a wide range of fine chemicals and micro/nano particles with processing times up to 10 min. The inter-dependency of mixing and residence times, and their direct correlation with reactor length have limited the adaptation of multiphase flow strategies for studies of processes with relatively long processing times (0.5–24 h). In this frontier article, we describe an oscillatory multiphase flow strategy to decouple mixing and residence times and enable investigation of longer timescale experiments than typically feasible with conventional continuous multiphase flow approaches. We review current oscillatory multiphase flow technologies, provide an overview of the advancements of this relatively new strategy in chemistry and biology, and close with a perspective on future opportunities.

 Received 6th June 2016,  
Accepted 1st July 2016

DOI: 10.1039/c6lc00728g

[www.rsc.org/loc](http://www.rsc.org/loc)

### Introduction

For several decades, researchers across multiple disciplines, particularly chemistry, biology, and engineering, have manipulated fluids at micro and milli-meter scale to prepare or analyze samples.<sup>1–4</sup> Shrinking the sample volume from milliliters to micro/nano liters, followed by further manipulation of the reagents in flow has enabled fundamental investigations and practical applications.<sup>5–8</sup> Single-phase continuous flow in sub millimeter channels was quickly realized to have challenges of unwanted Taylor dispersions, poor mixing and mass transfer as well as potential clogging by cells and particulates.<sup>9–12</sup> To circumvent these challenges, researchers separated the fluid of interest into small segments or fully entrapped segments within an inert continuous phase, which increased mixing and reduced (or completely avoided) contact with the channel walls.<sup>13–15</sup> One of the main promises of the resulting multiphase microfluidic technologies has been the “*high-throughput screening*”, that is, obtaining a large number of output parameters associated with different aspects of a process of interest in a faster and more efficient manner, compared to batch scale techniques (Fig. 1a).

A multitude of continuous multiphase microfluidic techniques have been developed for high-throughput studies of biological assays,<sup>16–20</sup> single cell encapsulation,<sup>21</sup> screening and optimization of protein crystallization,<sup>22,23</sup> picoinjections at kilohertz frequencies,<sup>24</sup> DNA/protein assays,<sup>25,26</sup> screening of photosensitizer activity,<sup>27</sup> kinetic studies of (bio)chemical

reactions,<sup>28</sup> screening of chemical reactions,<sup>29–34</sup> characterization of thermodynamic properties of gas–liquid processes,<sup>35–40</sup> and studies of micro/nanoparticle synthesis.<sup>41–53</sup> Different aspects of continuous multiphase microfluidics have already been discussed in multiple comprehensive reviews.<sup>13,15,54–56</sup> In this Frontier article, we first discuss challenges of continuous multiphase flow platforms for screening and optimization of (bio) chemical processes with long processing times. We then present a recently developed oscillatory multiphase flow approach based on oscillatory motion of a train of droplets dispersed in an inert continuous phase. Next, we introduce major experimental strategies for oscillatory multiphase flow. The review of the current state of oscillatory droplet-based strategies for high-throughput studies of relatively long chemical and biological processes is followed by our perspective on future directions and applications of this technology as a discovery platform in the fields of green chemistry, photo chemistry, and nanomaterials.

### Limitations of continuous multiphase flow

Continuous multiphase microfluidic approaches are proven to be fast and efficient platforms for screening and optimization of multi-parameter physical, chemical, and biological processes.<sup>16,25,27,41</sup> Nevertheless, inherent limitations associated with the constant length of a microchannel,  $L$ , (shown in Fig. 1b(i)) and the resulting dependence of the mixing timescale to the corresponding residence time through average flow velocity,<sup>57–59</sup> make it challenging to achieve similar mixing characteristics for varying processing times. Constant

Department of Chemical Engineering, Massachusetts Institute of Technology, 77 Massachusetts Avenue, 66-342, Cambridge, MA 02139, USA.  
E-mail: [kfjensen@mit.edu](mailto:kfjensen@mit.edu); Web: <http://web.mit.edu/jensenlab>



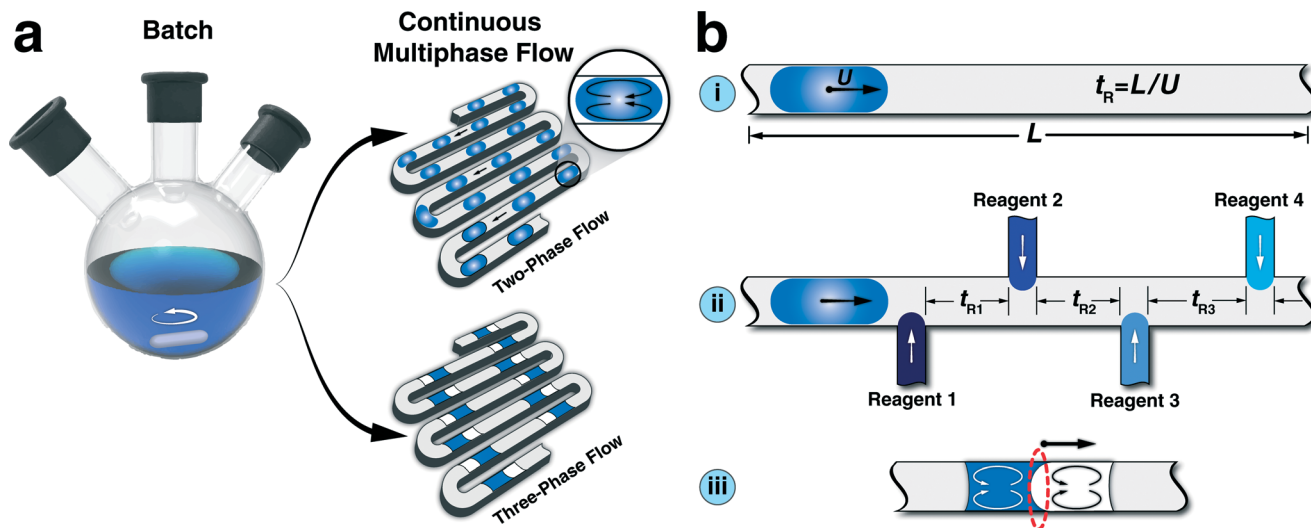


**Fig. 1** (a) Continuous multiphase flow strategy as an alternative for conventional batch processes. (b) Inherent challenges of continuous multiphase flow reactors for screening of physical, chemical, and biological processes: (i) limited residence time and direct correlation between mixing and reaction times due to the constant length of the reactor; (ii) in-series hard-wired residence times for multi-step processes; (iii) limited available interfacial area for bi-phasic interfacial reactions, highlighted in red, that is the semi-spherical cap between the two immiscible phases.

value of  $L$  limits the effective range of addressable residence times possible for a given set-up. Moreover, the hard-wired configuration of continuous multiphase flow strategies for multi-step processes (Fig. 1b(ii)) results in inter-dependency between the residence times of each step, and thereby complicates the systematic study of the effect of each step on the overall process performance (*i.e.*, separately varying residence times). In addition, the mass transfer limitation associated with the limited available interfacial area of three-phase flow formats (Fig. 1b(iii)) limits the studies of bi-phasic interfacial reactions (*e.g.*, C–C and C–N cross-coupling reactions). The aforementioned limitations could potentially be addressed by integration of a large number of external flow sensors, and development of multi-layer microfluidic network. However, it would be preferable to address limitations of continuous multiphase flow strategies without additional complexity.

One possible approach to achieve decoupling of mixing and residence times of continuous multiphase flow is stopping a train of pre-formed droplets either in microfabricated pockets<sup>60–62</sup> or sealed glass capillaries.<sup>63</sup> Stopping the flow of moving droplets would result in interfacial areas similar to continuous multiphase flow for bi-phasic processes, *without constant inter-phase stirring*. Furthermore, the stopped-flow strategy for droplets trapped within microfabricated pockets would often limit the characterization to a local read-out by optical microscopy.

A simple periodic reversal of flow direction addresses the aforementioned challenges and provides a modular flow strategy for characterization, screening, and optimization of processes with residence times ranging from seconds to hours. Examples of such processes include biphasic catalytic reactions,<sup>64</sup> colloidal nanomaterial synthesis,<sup>57,65</sup> monitoring bacterial growth,<sup>66,67</sup> cell-to-cell interaction,<sup>68</sup> and partition coefficient measurement of organic substances.<sup>69</sup>

## Oscillatory multiphase flow

### (A) Experimental strategies

Oscillation of a train of droplets (or a single droplet) in a micro/milli-fluidic channel can be achieved by applying an alternating pressure gradient on two ends of the channel. The alternating pressure gradient is typically realized through two experimental strategies; (a) computer-controlled electromagnetic valves (Fig. 2a) and (b) programmable syringe pumps with infuse/withdraw capabilities (Fig. 2b). In the first strategy, the inlet ports of the valves are connected to two different pressure sources (maintained at constant pressures), so that actuating the valves with a square waveform signal produces an oscillatory motion of pre-formed droplets within the flow reactor.<sup>57,67,70</sup> The pre-formed droplet(s) are

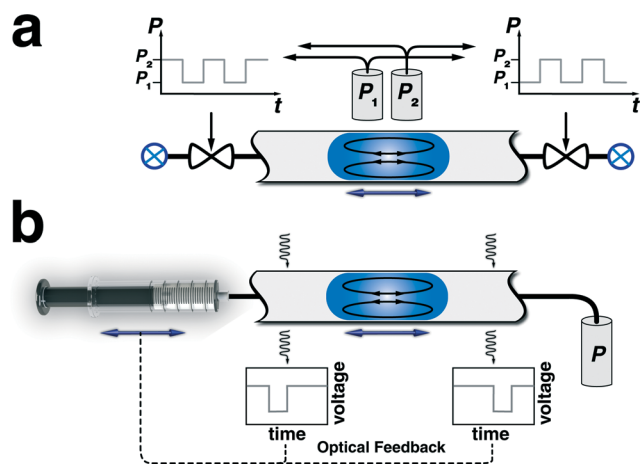


**Fig. 2** Schematic of two oscillatory flow strategies; (a) valve-based, and (b) syringe pump-based droplet oscillation approaches.



introduced into the reactor prior to the oscillatory actuation of electromagnetic valves. Furthermore, if needed, the droplets can be collected after a certain number of oscillation cycles for further off-line characterization.

In the second strategy, the alternating pressure gradient across the train of droplets is generated by switching the flow direction using a programmable syringe pump equipped with infuse/withdraw functionality, while maintaining the reactor outlet at a constant pressure.<sup>64,65,69,71</sup> The piston motion propagates through the carrier fluid and directly transfers the push/pull motion into oscillation of the pre-formed droplets.

In addition to the above-mentioned strategies, a combination of a 3-way electromagnetic valve, a constantly infusing syringe pump, and a closed microfluidic circuit can also be employed for oscillation of a train of droplets in a flow reactor.<sup>66,68</sup> In this approach, the inlet port of the 3-way electromagnetic valve is connected to a constantly infusing syringe pump, while the two outlet ports are connected to two sides of a closed-loop microfluidic circuit. Alternating the flow direction between the two sides of the channel *via* actuating the outlet ports of the computer-controlled valve generates the back-and-forth motion for the droplets trapped in the oscillatory zone of the microreactor.

It should also be noted that the range of addressable oscillation frequency,  $f$ , is defined by the employed experimental strategy. In the case of valve-based oscillatory multiphase flow strategy, oscillation frequencies up to 1 kHz have been achieved, which is due to the short response time of the electromagnetic valves ( $\sim 1$  ms).<sup>57</sup> In the case of syringe-pump based oscillatory multiphase flow approach, the maximum achievable oscillation frequency is defined by the mechanical syringe pump, which is usually limited to 1–10 Hz.<sup>64</sup>

### (B) Oscillatory mixing of miscible/immiscible fluids

The direct consequence of the oscillatory motion (shaking) of a droplet consisting of multiple miscible reagents is mixing of the fluids inside the droplet. The oscillatory motion of droplets (similar to the continuous multiphase flow) enhances the mixing and mass transfer as a result of recirculation zones<sup>72–74</sup> formed inside the droplets (Fig. 2). The presence of the axisymmetric recirculation patterns inside the slug reduces the characteristic diffusion length scale by the factor of two (*i.e.*, to quarter of the channel diameter). The direct correlation between the mixing timescale and the required reactor length associated with continuous multiphase flow reactors is removed in the oscillatory multiphase flow, since the droplet can be oscillated at a given speed to realize a particular degree of mixing and the number of oscillations can be adjusted to obtain the desired residence time. The parameter controlling the degree of mixing of two miscible fluids in the multiphase oscillatory flow strategy is the *stirring strength*, defined as  $S = fd/2(L_S + W)$ , where  $d$  is the distance travelled by the liquid segment during one full oscillation cycle,  $L_S$  is the length of the liquid segment, and  $W$  is the microchannel width.<sup>57</sup> Thus, the minimum oscillation amplitude (without sacrificing

mixing) for a shaking droplet is controlled by the required travel distance for a liquid droplet to form a complete recirculation pattern. Thulasidas *et al.*,<sup>75</sup> has previously demonstrated that the minimum travel distance for a complete recirculation inside a liquid droplet is three times of the total length of that droplet.



Fig. 3 (a) Microscale mixing of two immiscible fluids using oscillatory multiphase flow strategy for *in situ* studies of intra-phase transport processes. (b) Snapshot time-series of the oscillatory motion of a bi-phasic slug (clear phase: DI water, 15 μL, red phase: 1-octanol labelled with Sudan red, 10 μL, gas: pressurized nitrogen) in a tubular FEP reactor, during one complete oscillation cycle. (c) Ideal microscale mixing of two immiscible fluids using oscillatory multiphase flow strategy for *in-flow* studies of bi-phasic interfacial catalytic reactions. The available interfacial area for the multiphase process is highlighted in red. Adopted with permission from the American Chemical Society, 2015 (b).<sup>69</sup>





In addition to mixing of two miscible fluids, oscillatory multiphase flow strategy also allows for operation of processes involving two immiscible fluids (Fig. 3). Examples of multiphase processes include interfacial catalytic reactions and intra-phase transport of solute molecules (e.g., liquid–liquid extraction). For chemical reactions occurring at an aqueous–organic interface (e.g., bi-phasic cross-coupling reactions), it is desirable to maximize the available interfacial area over the course of the oscillatory flow experiment. The ordered arrangement of two immiscible fluids, as shown in Fig. 1b(iii) results in a limited available interfacial area for interfacial chemical reactions. However, tuning the surface energy of the aqueous and organic phase segments of the bi-phasic slug on the reactor wall *via* changing the reactor material,<sup>76,77</sup> can enhance the available interfacial area for a desired multiphase process. For multiphase processes involving intra-phase transport of solute molecules (e.g., liquid–liquid extraction), in addition to the full engulfment of the aqueous phase within the organic phase, it is desirable to achieve complete separation of the two phases at each oscillation cycle, allowing for *in situ* optical characterization of each phase individually for studies of the intra-phase transport process.

As shown in Fig. 3a(I), in the initial bi-phasic slug configuration, both aqueous and organic phases are wetting the Teflon reactor. Upon starting the flow direction from left to right, the higher surface energy of the aqueous phase on the Teflon reactor, compared to the organic phase, results in a more facile motion of the aqueous segment. The unbalanced surface tension forces at the three-phase contact line in combination with the higher surface energy of the aqueous phase to the organic phase on the Teflon reactor, as well as the relatively low bi-phasic interfacial area results in engulfment of the aqueous phase within the organic phase. Upon full engulfment of the aqueous segment within the organic segment, the lubrication film (organic phase) surrounding the aqueous phase, results in a higher velocity for the engulfed aqueous phase (Fig. 3a(II) and b). The higher average velocity of the engulfed aqueous phase, compared to the wetting organic phase results in the relative displacement of the engulfed aqueous droplet from the back to the front of the organic segment, shown in the time-series of bright-field images of one complete oscillation cycle for a bi-phasic slug comprising DI water (clear phase) and 1-octanol (red phase).<sup>69</sup> Ultimately, due the higher velocity of the engulfed phase, the aqueous droplet exits the wetting organic phase, wets the reactor wall, and the bi-phasic slug becomes two separate phases, both wetting the Teflon reactor (Fig. 3a(III) and b). The separation of two phases into two distinct segments (*i.e.*, removal of the lubrication film), enables *in situ* absorption spectroscopy of each phase without interference of the other phase at each oscillation cycle.

In order to achieve maximum available interfacial area for bi-phasic catalytic reactions, ideally, the aqueous phase of the bi-phasic slug should be constantly engulfed within the organic phase throughout the experiment (Fig. 3c). Employing the scaling law relationship between the lubrication

film thickness and the Capillary number of the aqueous phase,<sup>78,79</sup> the minimum required oscillatory flow velocity,  $U_{th}$ , to achieve full engulfment of the aqueous phase within the organic phase during each oscillation cycle can be analytically predicted,<sup>64</sup>

$$U_{th} = \left( \frac{d_{rel}}{m(d + d_{rel})} \right)^{3/2} \left( \frac{\sigma}{\mu} \right) \left( \frac{d}{d + d_{rel}} \right)$$

where  $d_{rel}$  is the relative displacement between the engulfed aqueous droplet and wetting organic segment,  $d$  is the oscillation amplitude,  $\sigma$  is the bi-phasic interfacial tension,  $\mu$  is the viscosity of the aqueous phase, and  $m$  is a fitting parameter.

It should also be noted that for processes operating at temperatures higher than room temperature, the temperature gradient between the oscillatory zone of the reactor and the remaining fluidic network might cause drifting of the train of droplets due to thermocapillarity motion<sup>80,81</sup> or change in the density of the carrier fluid (gas) over the course of the experiment. Integration of an external optical feedback strategy (e.g., absorbance of a collimated light passing through a fluidic channel) can provide a reliable real-time information for automatic switching of the flow direction, thereby avoiding the drifting of the droplets from the heated zone of the flow reactor during the oscillation (Fig. 2b).

## Applications of oscillatory multiphase flow platforms

### (A) Chemistry

The oscillatory motion of an aqueous droplet was originally employed for mixing of two pre-formed droplets in a PDMS-based microfluidic channel (using air as the continuous phase), shown in Fig. 4a. The designed microfluidic platform was then utilized for *in situ* studies of an enzymatic reaction between L-glutamate oxidase and horseradish peroxidase through fluorescence microscopy.<sup>82</sup> Computer-controlled microsyringe pumps with pre-defined infuse/withdraw volumes were employed for metering, sorting, merging, and oscillatory motion of a train of aqueous droplets containing different concentrations of L-glutamate. It was found that the activity of L-glutamate oxidase was highest in a pH range between 7 and 8 and further decrease or increase of pH gradually decrease its activity. This early oscillatory multiphase flow platform demonstrated the advantages of discretized residence/reaction times for process control using droplets in fluidic network. The on-demand control of the droplet position within the microchannel was similar to the precise level of droplet control obtained in electrowetting-based microfluidic devices<sup>83</sup> (*i.e.*, digital microfluidics), without the need for applying localized electronic potential.

Dolega *et al.*<sup>70</sup> developed a valve-based oscillatory multiphase flow, using paraffin oil as the carrier fluid, for on-chip screening and evaluation of proteins solubility diagrams (Fig. 4b), *via* an integrated spectral characterization



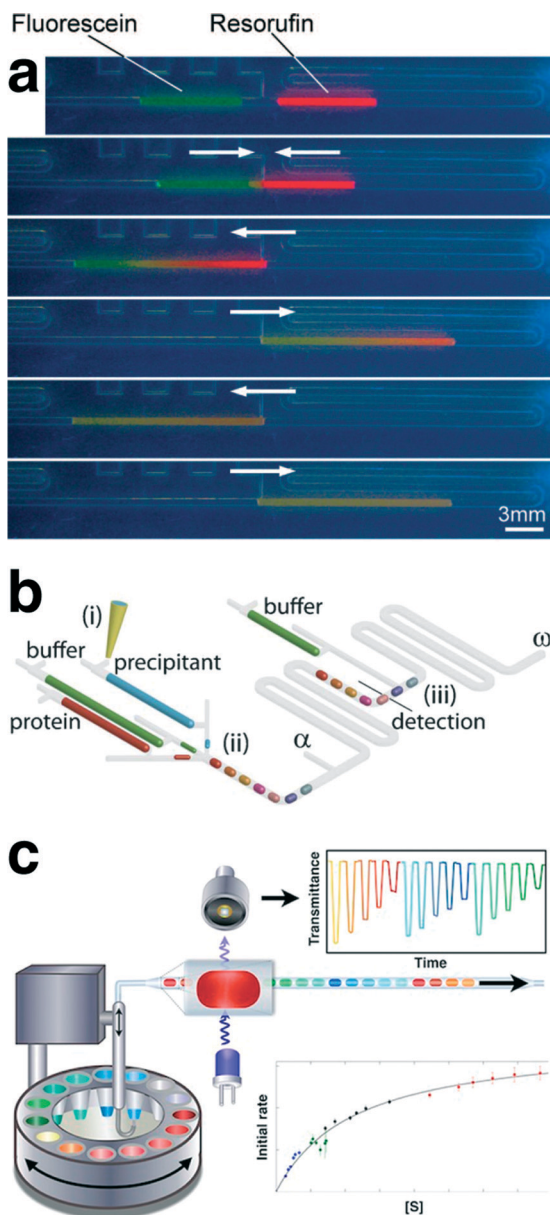


**Fig. 4** (a) Merging and mixing of two on-chip metered aqueous microdroplets using air-driven oscillatory motion characterized by fluorescence microscopy. (b) Schematic of the automated oscillatory multiphase flow strategy for continuous observation of crystallization process within oscillating droplets. (c) Schematic of the automated compartment-on-demand setup, developed for studies of enzyme kinetics and inhibition. Reproduced with permissions from the American Chemical Society, 2008 (a),<sup>82</sup> and 2013 (c)<sup>71</sup> and the Royal Society of Chemistry, 2012 (b).<sup>70</sup>

tool (UV-vis absorption spectroscopy).<sup>70</sup> A train of 30 aqueous droplets (960 nL per droplet) containing different concentration ratios of lysozyme and precipitant solutions were formed, and their corresponding UV absorption spectra were monitored every 15 min for an overall experiment time of 5 h. The automated oscillatory multiphase flow platform was then used to determine the lysozyme solubility diagrams as a function of concentrations of protein and precipitant. This

work, for the first time, demonstrated the applicability of multiphase flow strategies for studies of long-term chemical processes (>30 min).

In a different multiphase oscillatory flow setup, a computer-controlled syringe pump integrated with a robotic arm and an in-line absorbance flow cell was used for on-demand formation and oscillation of microdroplets in a PTFE tubing from multiple aqueous reservoirs immersed in

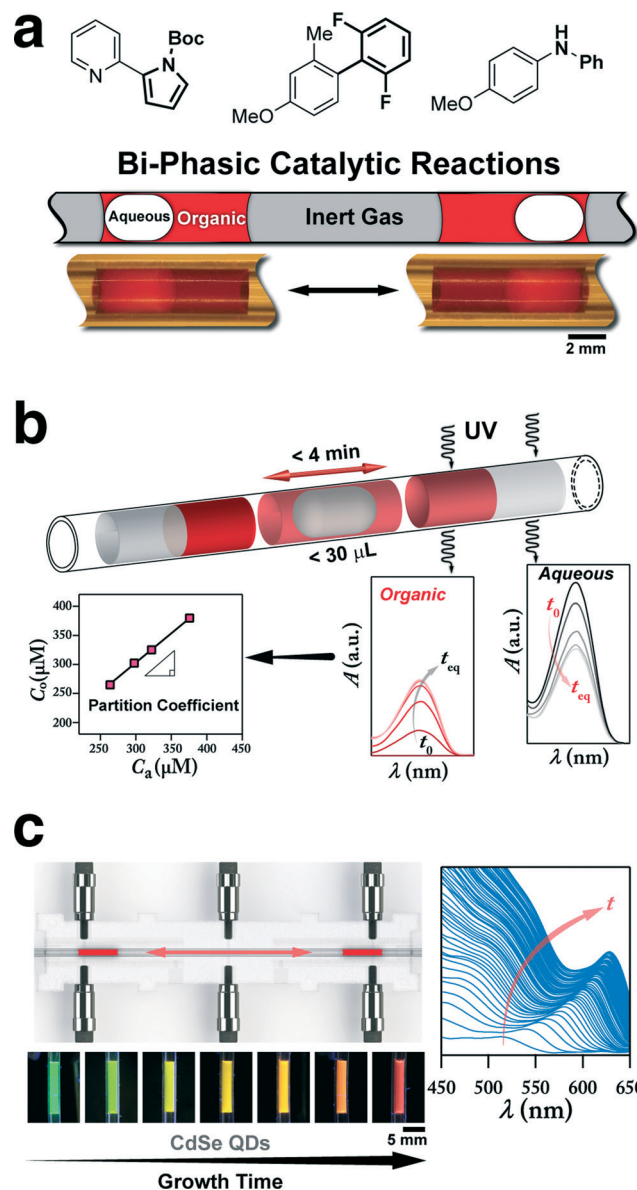


**Fig. 5** (a) Three-phase oscillatory flow reactor for in-flow studies of bi-phasic interfacial catalytic reactions (e.g., C-C and C-N cross-coupling reactions). (b) Oscillatory multiphase flow strategy integrated with *in situ* UV absorption spectroscopy for fast and efficient water-octanol partition coefficient measurement and screening of organic compounds. The continuous phase is pressurized nitrogen (10 psig). (c) Oscillatory microprocessor for *in situ* characterization of the growth of semiconductor nanocrystals at the synthesis temperature. Reprinted with permission from the Royal Society of Chemistry, 2015 (a)<sup>64</sup> and the American Chemical Society, 2015 (b)<sup>69</sup> and (c).<sup>65</sup>



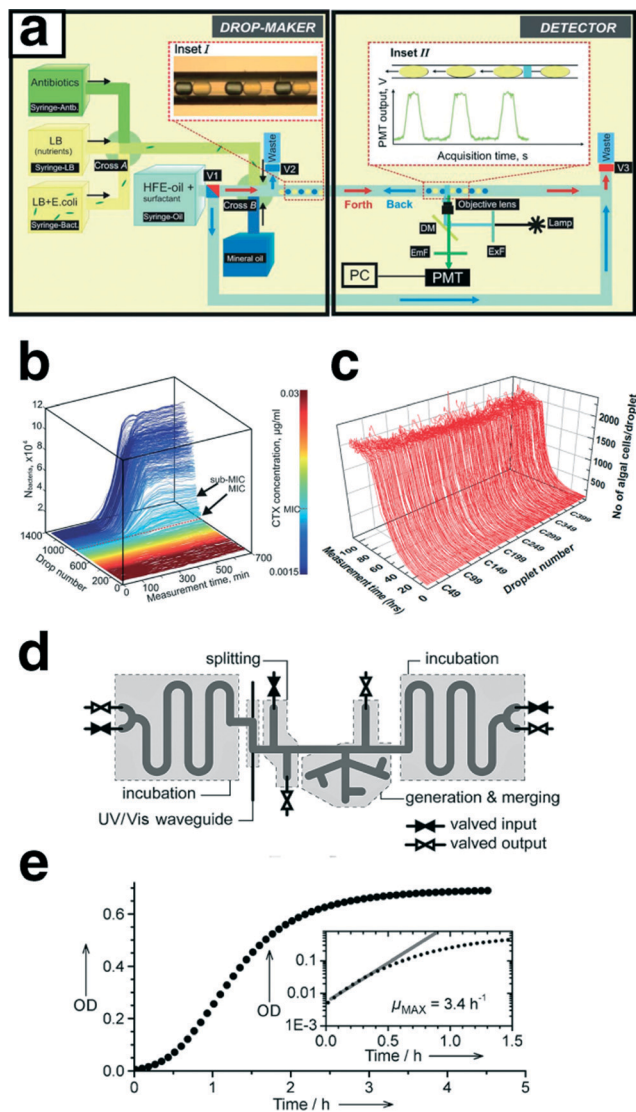


**Fig. 6** (a) Automated millifluidic platform developed for continuous monitoring of the growth dynamics of microbial populations over multiple generations; the setup includes droplet generation, incubation, and characterization *via* oscillatory motion of the pre-formed droplets. (b) 3-D growth curves of the bacterial populations, grown in the gradient of antibiotic cefotaxime (CTX) concentrations. (c) 3-D growth curves of 450 microdroplets with initial inoculation population size of  $\sim 100$  unicellular microalgae *C. reinhardtii* cells per droplet. (d) Schematic of the designed and microfabricated microfluidic device for long-term continuous observation of population growth of bacteria. (e) Growth curve of *E. coli* ATCC 25992 cells obtained using the microdroplet-based chemostat shown in (d). Reproduced with permission from the Royal Society of Chemistry, 2011 (a, b),<sup>66</sup> from Public Library of Science, 2015 (c)<sup>68</sup> and from Wiley-VCH, 2013 (d, e).<sup>67</sup>

an inert continuous phase (Fig. 4c).<sup>71</sup> The automated compartment on-demand platform was then utilized to conduct nanoliter assays in a high-throughput manner to obtain Michaelis–Menten parameters associated with hydrolysis of 4-nitrophenyl glucopyranoside by sweet almond  $\beta$ -glucosidase using a total sample volume of only 1.4  $\mu$ L. In addition, the kinetic parameters of the inhibition of the enzymatic reaction

of 1-deoxynojirimycin and conduritol B epoxide were measured within 20 min. This work further demonstrated the application of oscillatory multiphase flow strategy for obtaining a large data set of the process of interest accommodated within a short reactor length (volume).

In a different study, two 3-port electromagnetic valves connected to two constant pressure sources of the dispersed phase (gas) were employed for alternating the pressure gradient applied across a train of droplets within a hybrid silicon-Pyrex microfluidic device.<sup>57</sup> Microscale mixing of two miscible fluids within a liquid segment enabled by the oscillatory multiphase flow format was characterized using fluorescence microscopy. In addition, integrating on-chip UV-vis absorption spectroscopy with oscillatory flow allowed long-term studies of the size and shape evolution of metallic nanoparticles (gold nanorods). The transverse and longitudinal surface plasmon resonance absorbance peaks associated with diameter and length of the gold nanorods, respectively, were monitored for on-line evaluation of the shape evolution kinetics over the course of a 5 h chemical etching process.

Recently, a syringe-pump based oscillatory flow strategy using pressurized inert gas as the carrier phase in combination with a computer-controlled liquid handler was developed for in-flow studies of chemical processes comprising immiscible fluids (Fig. 5a and b).<sup>64,69</sup> Integration of in-line analytical tools such as UV-vis absorption spectroscopy, HPLC, and mass spectroscopy units with the developed multiphase oscillatory flow strategy enabled screening, library development, and optimization of the physical/chemical process of interest. The developed oscillatory multiphase flow strategy was then applied for in-flow studies of bi-phasic Suzuki–Miyaura and Buchwald–Hartwig cross coupling reactions<sup>64</sup> (Fig. 5a), as well as automated measurement and screening of water-octanol partition coefficient of pharmaceutical compounds<sup>69</sup> (Fig. 5b). The increase in the available interfacial area, owing to the complete engulfment of the aqueous droplet within the organic phase (Fig. 5a), addressed the mass transfer limitation of continuous multiphase flow strategies for studies of bi-phasic C–C and C–N cross coupling reactions, and reproduced the same reaction yields as a batch reactor. As explained before, in the oscillatory micromixing of two immiscible fluids (Fig. 3), the higher surface energy of the aqueous phase on the Teflon reactor, compared to the organic phase, results in a more facile motion of the aqueous phase and full engulfment of the aqueous droplet within the wetting organic segment. The presence of the organic phase lubrication film surrounding the aqueous phase, results in a higher velocity for the engulfed aqueous phase (Fig. 5b), and displacement of the engulfed aqueous droplet from the back to the front of the wetting organic phase.

On the other hand, use of an integrated optical feedback strategy (through two fiber-coupled LEDs and photodetectors) avoided drifting and ensured the pre-formed droplet was trapped within the heated region of the oscillatory flow reactor for the intended processing time. Combination of the optical feedback with an *in situ* UV-vis absorption spectroscopy





technique enabled automated water–octanol partition coefficient measurement of pharmaceutical compounds within 4 min per drug at the physiologically relevant temperature of 37 °C, which is otherwise time-and labour-intensive to obtain using conventional batch scale techniques (e.g., shake-flask method).<sup>69</sup>

A similar oscillatory flow platform was used to study growth of II–VI and III–V semiconductor nanocrystals at relatively high temperatures (160–220 °C).<sup>65</sup> The temporal *in situ* measurements of absorption spectra for the semiconductor nanocrystals at the synthesis temperature, shown in Fig. 5c, provided insights into the effect of synthesis temperature on growth kinetics.

## (B) Biology

In addition to physical and chemical processes, the multiphase oscillatory flow technique has enabled long-term studies of biological processes. A combination of a constantly infusing syringe pump and a computer-controlled electric valve was implemented in a liquid–liquid oscillatory multiphase flow platform for high-throughput long-term studies of the dynamics of microbial population growth.<sup>66</sup> The population growth was monitored over multiple generations in >1000 droplets (~100 nL per droplet), shown in Fig. 6a and b.<sup>66</sup> The automated millifluidic setup was then used in systematic studies of the effect of medium composition on the growth rate of microbial population. In addition, the doubling times of monoclonal populations of *E. coli* were automatically determined through monitoring minimal inhibitory concentration of an antibiotic cefotaxime (CTX) using fluorescence microscopy (Fig. 6b). A similar oscillatory flow platform was also employed to study the effect of cell-to-

cell heterogeneity on growth dynamics of isogenic cell populations of *Chlamydomonas reinhardtii* over a period of one week (Fig. 6c). The millifluidic setup was capable of sorting and collecting the droplets of interest containing viable cells at the end of the experiment for further off-line characterization.<sup>68</sup> To avoid cross-contamination between the adjacent droplets over the course of a 100 h experiment, an inert droplet (air) was inserted between each two consecutive aqueous droplets containing the microalgae cells dispersed in tris-acetate–phosphate (TAP, growth solution). The oscillatory motion of droplets, in addition to ensuring homogenous distribution of dissolved oxygen and carbon dioxide within droplets, prevented the settling and aggregation of algal cells through constant stirring and internal recirculation. Fig. 6c shows homogenous growth dynamics of *Chlamydomonas* cells from an initial population size of ~100 cells per droplet, obtained *via* fluorescence microscopy. These work demonstrated another avenue for utilization of oscillatory multiphase flow strategy in long-term studies of biological processes as a high-throughput nanoliter assay. In another microbiology study, Jakiela *et al.*<sup>67</sup> developed a valve-based oscillatory flow platform for manipulation and continuous monitoring of population growth of bacteria in microdroplet chemostats, through *in situ* spectral characterization (Fig. 6d).<sup>67</sup>

The automated microdroplet chemostat setup allowed on-demand formation of microdroplets containing *E. coli* cells and growth factors. The on-chip formed microdroplet chemostats (164 droplets) were then cycled back and forth for incubation and continuous population monitoring (Fig. 6e).

Discretizing the motion of microdroplets through computer-controlled electromagnetic valves enabled on-demand addition (infusion) of chemical factors to the

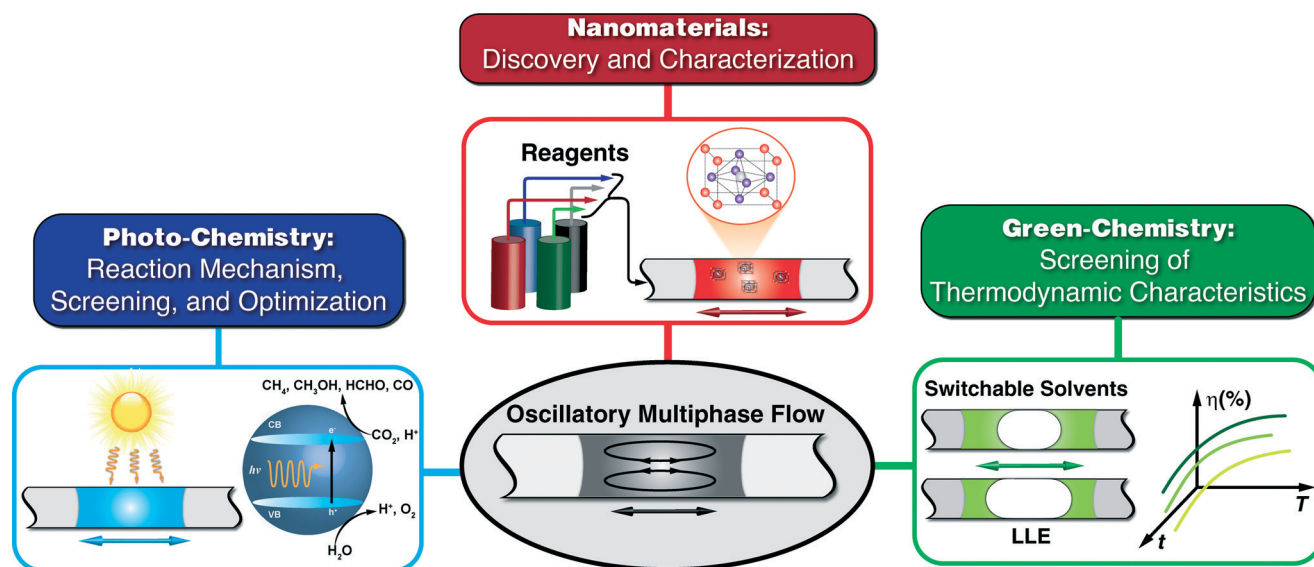


**Fig. 7** Proposed future opportunities of oscillatory multiphase flow strategy (a) as a discovery and characterization platform for targeted development of the next generation of semiconductor/metallic nanomaterials in solar cells, displays, and biological imaging; (b) as an experimental strategy for fundamental studies of photo-chemical CO<sub>2</sub> reduction and visible-light photo-redox catalysis processes; (c) as a high-throughput screening platform for thermodynamic studies of CO<sub>2</sub>-triggered switchable solvents (switchable ionic strength, polarity, and hydrophilicity).



microdroplet chemostats over the course of the experiment. The automated micro-chemostat platform demonstrated a multi-step operation (*i.e.*, on-demand composition tuning of the microdroplets) enabled through oscillatory flow strategy. The ability to constantly provide fresh nutrients to microdroplets extended the long-term parallel studies of the effect of varying chemical factors on the dynamics of microbial populations to over 100 h.

## Summary and outlook

Oscillatory multiphase flow techniques over the past couple of years have demonstrated the possibility of adaptation of microscale flow technologies for studies of long-term (>30 min) physical, chemical, and biological processes by addressing the residence time limitation associated with continuous multiphase flow strategies. Moreover, the simple back-and-forth motion of droplets has enabled single-point temporal characterization of the process of interest within the micro-reaction vessel (*i.e.*, microdroplet) through *in situ* UV-vis spectroscopy at the relevant pressures and temperatures, without the need for manual sampling or formation of single droplet per reaction time. A single microdroplet could be used for kinetic studies of the (bio)chemical reaction at a defined temperature, pressure, and concentration. In addition, multiplexed oscillatory multiphase flow platforms could be envisioned for high-throughput parameter screening of gas/liquid-liquid reactions in a numbered up reactor configuration, operating at different temperatures to surpass conventional batch scale and well-plate based high-throughput screening strategies operated at a constant temperature.

The oscillatory multiphase flow strategy has the potential to become a versatile and efficient discovery and characterization tool in long-term studies of (bio)chemical processes, but a number of important questions remain to be addressed.

The oscillatory flow approach would greatly benefit from further hydrodynamic characterization of single/multi-phase flow formats. A comprehensive guideline suggesting the reactor material (based on the desired surface energy, and flow behaviour) for the target application would accelerate the future development of the technology. Furthermore, reducing the number of custom-designed parts and utilizing commercially available off-the-shelf components (*e.g.*, tubing and fluidic connectors instead of microfabricated reactors) would facilitate further adaptation of the oscillatory multiphase flow setup in chemistry and biology research labs. Additionally, providing detailed carry-over characterization, and potential experimental strategies (*e.g.*, washing protocols) to significantly reduce (or completely remove) the effect of droplets carry-over on the measured results would be beneficial.

In addition to the case studies highlighted in this frontier article, as shown in Fig. 7, we envision that the modular and easy to assemble oscillatory multiphase flow technique could potentially be applied towards better fundamental understanding of (a) nanomaterials of future for energy, biology,

and display applications (*e.g.*, organometal halide perovskite nanocrystals,<sup>84</sup> and rare earth upconversion nanocrystals<sup>85</sup>); (b) photocatalytic reactions such as visible light photo-redox catalysis<sup>86</sup> and photochemical reduction of carbon dioxide; (c) solvent extraction kinetics and recovery efficiency of the recently developed CO<sub>2</sub>-triggered switchable solvents (*e.g.*, nitrogenous bases), as green alternatives to volatile and toxic organic solvents.<sup>87,88</sup>

In summary, continuous multiphase flow has significantly improved the accuracy and throughput of conventional discovery and screening methodologies in chemistry and biology. Capitalizing on the separation of characteristic mixing and residence time scales, oscillatory multiphase flow technology further expands and complements the addressable parameter space associated with continuous multiphase flow approaches. We hope this frontier article will further facilitate the adaptation of oscillatory microscale flow strategies in pharma, energy, and healthcare sectors as a reliable and an efficient discovery and exploratory platform.

## Acknowledgements

M. A. gratefully acknowledges financial support from an NSERC Postdoctoral Fellowship.

## References

- 1 G. M. Whitesides, *Nature*, 2006, **442**, 368–373.
- 2 A. J. deMello, *Nature*, 2006, **442**, 394–402.
- 3 G. M. Whitesides, *Nat. Biotechnol.*, 2003, **21**, 1161–1165.
- 4 J. El-Ali, P. K. Sorger and K. F. Jensen, *Nature*, 2006, **442**, 403–411.
- 5 T. M. Squires and S. R. Quake, *Rev. Mod. Phys.*, 2005, **77**, 977–1026.
- 6 K. S. Elvira, X. C. I. Solvas, R. C. R. Wootton and A. J. deMello, *Nat. Chem.*, 2013, **5**, 905–915.
- 7 K. F. Jensen, *Chem. Eng. Sci.*, 2001, **56**, 293–303.
- 8 R. L. Hartman, J. P. McMullen and K. F. Jensen, *Angew. Chem., Int. Ed.*, 2011, **50**, 7502–7519.
- 9 Y. Kikutani and T. Kitamori, *Macromol. Rapid Commun.*, 2004, **25**, 158–168.
- 10 S. L. Poe, M. A. Cummings, M. P. Haaf and D. T. McQuade, *Angew. Chem., Int. Ed.*, 2006, **45**, 1544–1548.
- 11 H. A. Stone and S. Kim, *AIChE J.*, 2001, **47**, 1250–1254.
- 12 S. Marre and K. F. Jensen, *Chem. Soc. Rev.*, 2010, **39**, 1183–1202.
- 13 H. Song, D. L. Chen and R. F. Ismagilov, *Angew. Chem., Int. Ed.*, 2006, **45**, 7336–7356.
- 14 S.-Y. Teh, R. Lin, L.-H. Hung and A. P. Lee, *Lab Chip*, 2008, **8**, 198–220.
- 15 A. Gunther and K. F. Jensen, *Lab Chip*, 2006, **6**, 1487–1503.
- 16 M. T. Guo, A. Rotem, J. A. Heyman and D. A. Weitz, *Lab Chip*, 2012, **12**, 2146–2155.
- 17 J. J. Agresti, E. Antipov, A. R. Abate, K. Ahn, A. C. Rowat, J.-C. Baret, M. Marquez, A. M. Klibanov, A. D. Griffiths and D. A. Weitz, *Proc. Natl. Acad. Sci. U. S. A.*, 2010, **107**, 4004–4009.





- 18 B. L. Wang, A. Ghaderi, H. Zhou, J. Agresti, D. A. Weitz, G. R. Fink and G. Stephanopoulos, *Nat. Biotechnol.*, 2014, **32**, 473–478.
- 19 E. Brouzes, M. Medkova, N. Savenelli, D. Marran, M. Twardowski, J. B. Hutchison, J. M. Rothberg, D. R. Link, N. Perrimon and M. L. Samuels, *Proc. Natl. Acad. Sci. U. S. A.*, 2009, **106**, 14195–14200.
- 20 C. B. Rohde, F. Zeng, R. Gonzalez-Rubio, M. Angel and M. F. Yanik, *Proc. Natl. Acad. Sci. U. S. A.*, 2007, **104**, 13891–13895.
- 21 M. Chabert and J.-L. Viovy, *Proc. Natl. Acad. Sci. U. S. A.*, 2008, **105**, 3191–3196.
- 22 L. Li, D. Mustafi, Q. Fu, V. Tereshko, D. L. Chen, J. D. Tice and R. F. Ismagilov, *Proc. Natl. Acad. Sci. U. S. A.*, 2006, **103**, 19243–19248.
- 23 L. Li and R. F. Ismagilov, *Annu. Rev. Biophys.*, 2010, **39**, 139–158.
- 24 A. R. Abate, T. Hung, P. Mary, J. J. Agresti and D. A. Weitz, *Proc. Natl. Acad. Sci. U. S. A.*, 2010, **107**, 19163–19166.
- 25 M. Srisa-Art, A. J. deMello and J. B. Edel, *Anal. Chem.*, 2007, **79**, 6682–6689.
- 26 J.-W. Choi, D.-K. Kang, H. Park, A. J. deMello and S.-I. Chang, *Anal. Chem.*, 2012, **84**, 3849–3854.
- 27 S. Cho, D.-K. Kang, S. Sim, F. Geier, J.-Y. Kim, X. Niu, J. B. Edel, S.-I. Chang, R. C. R. Wootton, K. S. Elvira and A. J. deMello, *Anal. Chem.*, 2013, **85**, 8866–8872.
- 28 M. Srisa-Art, E. C. Dyson, A. J. deMello and J. B. Edel, *Anal. Chem.*, 2008, **80**, 7063–7067.
- 29 K. Churski, P. Korczyk and P. Garstecki, *Lab Chip*, 2010, **10**, 816–818.
- 30 K. Churski, T. S. Kaminski, S. Jakiela, W. Kamysz, W. Baranska-Rybak, D. B. Weibel and P. Garstecki, *Lab Chip*, 2012, **12**, 1629–1637.
- 31 T. S. Kaminski, S. Jakiela, M. A. Czekalska, W. Postek and P. Garstecki, *Lab Chip*, 2012, **12**, 3995–4002.
- 32 J. Guzowski, P. M. Korczyk, S. Jakiela and P. Garstecki, *Lab Chip*, 2011, **11**, 3593–3595.
- 33 D. Chen, W. Du, Y. Liu, W. Liu, A. Kuznetsov, F. E. Mendez, L. H. Philipson and R. F. Ismagilov, *Proc. Natl. Acad. Sci. U. S. A.*, 2008, **105**, 16843–16848.
- 34 B. J. Reizman and K. F. Jensen, *Chem. Commun.*, 2015, **51**, 13290–13293.
- 35 M. Abolhasani, M. Singh, E. Kumacheva and A. Gunther, *Lab Chip*, 2012, **12**, 1611–1618.
- 36 D. Voicu, M. Abolhasani, R. Choueiri, G. Lestari, C. Seiler, G. Menard, J. Greener, A. Guenther, D. W. Stephan and E. Kumacheva, *J. Am. Chem. Soc.*, 2014, **136**, 3875–3880.
- 37 M. Abolhasani, A. Günther and E. Kumacheva, *Angew. Chem., Int. Ed.*, 2014, **53**, 7992–8002.
- 38 G. Lestari, M. Abolhasani, D. Bennett, P. Chase, A. Günther and E. Kumacheva, *J. Am. Chem. Soc.*, 2014, **136**, 11972–11979.
- 39 S. G. R. Lefortier, P. J. Hamersma, A. Bardow and M. T. Kreutzer, *Lab Chip*, 2012, **12**, 3387–3391.
- 40 R. Sun and T. Cubaud, *Lab Chip*, 2011, **11**, 2924–2928.
- 41 G. Niu, A. Ruditskiy, M. Vara and Y. Xia, *Chem. Soc. Rev.*, 2015, **44**, 5806–5820.
- 42 L. Zhang, G. Niu, N. Lu, J. Wang, L. Tong, L. Wang, M. J. Kim and Y. Xia, *Nano Lett.*, 2014, **14**, 6626–6631.
- 43 I. Lignos, L. Protesescu, S. Stavrakis, L. Piveteau, M. J. Speirs, M. A. Loi, M. V. Kovalenko and A. J. deMello, *Chem. Mater.*, 2014, **26**, 2975–2982.
- 44 I. Lignos, S. Stavrakis, G. Nedelcu, L. Protesescu, A. J. deMello and M. V. Kovalenko, *Nano Lett.*, 2016, **16**, 1869–1877.
- 45 A. M. Nightingale, T. W. Phillips, J. H. Bannock and J. C. de Mello, *Nat. Commun.*, 2014, **5**, 3777.
- 46 A. R. C. Duarte, B. Ünal, J. F. Mano, R. L. Reis and K. F. Jensen, *Langmuir*, 2014, **30**, 12391–12399.
- 47 S. Xu, Z. Nie, M. Seo, P. Lewis, E. Kumacheva, H. A. Stone, P. Garstecki, D. B. Weibel, I. Gitlin and G. M. Whitesides, *Angew. Chem., Int. Ed.*, 2005, **44**, 724–728.
- 48 Z. Nie, W. Li, M. Seo, S. Xu and E. Kumacheva, *J. Am. Chem. Soc.*, 2006, **128**, 9408–9412.
- 49 S.-K. Lee, J. Baek and K. F. Jensen, *Langmuir*, 2014, **30**, 2216–2222.
- 50 V. Sebastian, C. D. Smith and K. F. Jensen, *Nanoscale*, 2016, **8**, 7534–7543.
- 51 S. Duraiswamy and S. A. Khan, *Small*, 2009, **5**, 2828–2834.
- 52 S. A. Khan, A. Günther, M. A. Schmidt and K. F. Jensen, *Langmuir*, 2004, **20**, 8604–8611.
- 53 B. K. H. Yen, A. Günther, M. A. Schmidt, K. F. Jensen and M. G. Bawendi, *Angew. Chem.*, 2005, **117**, 5583–5587.
- 54 A. B. Theberge, F. Courtois, Y. Schaerli, M. Fischlechner, C. Abell, F. Hollfelder and W. T. S. Huck, *Angew. Chem., Int. Ed.*, 2010, **49**, 5846–5868.
- 55 A. Huebner, S. Sharma, M. Srisa-Art, F. Hollfelder, J. B. Edel and A. J. deMello, *Lab Chip*, 2008, **8**, 1244–1254.
- 56 D. T. Chiu, R. M. Lorenz and G. D. M. Jeffries, *Anal. Chem.*, 2009, **81**, 5111–5118.
- 57 M. Abolhasani, A. Oskooei, A. Klinkova, E. Kumacheva and A. Gunther, *Lab Chip*, 2014, **14**, 2309–2318.
- 58 V. S. Chakravarthy and J. M. Ottino, *Chem. Eng. Sci.*, 1996, **51**, 3613–3622.
- 59 W.-L. Chien, H. Rising and J. M. Ottino, *J. Fluid Mech.*, 1986, **170**, 355–377.
- 60 F. Shen, W. Du, J. E. Kreutz, A. Fok and R. F. Ismagilov, *Lab Chip*, 2010, **10**, 2666–2672.
- 61 D. E. Cohen, T. Schneider, M. Wang and D. T. Chiu, *Anal. Chem.*, 2010, **82**, 5707–5717.
- 62 Y. Wang, Y. Li, H. Thérien-Aubin, J. Ma, P. W. Zandstra and E. Kumacheva, *Biomicrofluidics*, 2016, **10**, 014110.
- 63 C. J. Gerdt, V. Tereshko, M. K. Yadav, I. Dementieva, F. Collart, A. Joachimiak, R. C. Stevens, P. Kuhn, A. Kossiakoff and R. F. Ismagilov, *Angew. Chem., Int. Ed.*, 2006, **45**, 8156–8160.
- 64 M. Abolhasani, N. C. Bruno and K. F. Jensen, *Chem. Commun.*, 2015, **51**, 8916–8919.
- 65 M. Abolhasani, C. W. Coley, L. Xie, O. Chen, M. G. Bawendi and K. F. Jensen, *Chem. Mater.*, 2015, **27**, 6131–6138.
- 66 L. Baraban, F. Bertholle, M. L. M. Salverda, N. Bremond, P. Panizza, J. Baudry, J. A. G. M. de Visser and J. Bibette, *Lab Chip*, 2011, **11**, 4057–4062.



- 67 S. Jakiela, T. S. Kaminski, O. Cybulski, D. B. Weibel and P. Garstecki, *Angew. Chem., Int. Ed.*, 2013, **52**, 8908–8911.
- 68 S. P. Damodaran, S. Eberhard, L. Boitard, J. G. Rodriguez, Y. Wang, N. Bremond, J. Baudry, J. Bibette and F.-A. Wollman, *PLoS One*, 2015, **10**, e0118987.
- 69 M. Abolhasani, C. W. Coley and K. F. Jensen, *Anal. Chem.*, 2015, **87**, 11130–11136.
- 70 M. E. Dolega, S. Jakiela, M. Razew, A. Rakszewska, O. Cybulski and P. Garstecki, *Lab Chip*, 2012, **12**, 4022–4025.
- 71 F. Gielen, L. van Vliet, B. T. Koprowski, S. R. A. Devenish, M. Fischlechner, J. B. Edel, X. Niu, A. J. deMello and F. Hollfelder, *Anal. Chem.*, 2013, **85**, 4761–4769.
- 72 S. Jakiela, P. M. Korczyk, S. Makulska, O. Cybulski and P. Garstecki, *Phys. Rev. Lett.*, 2012, **108**, 134501.
- 73 C. N. Baroud, F. Gallaire and R. Danga, *Lab Chip*, 2010, **10**, 2032–2045.
- 74 H. Kinoshita, S. Kaneda, T. Fujii and M. Oshima, *Lab Chip*, 2007, **7**, 338–346.
- 75 T. C. Thulasidas, M. A. Abraham and R. L. Cerro, *Chem. Eng. Sci.*, 1995, **50**, 183–199.
- 76 J. Bico and D. Queré, *J. Fluid Mech.*, 2002, **467**, 101–127.
- 77 D. L. Chen, L. Li, S. Reyes, D. N. Adamson and R. F. Ismagilov, *Langmuir*, 2007, **23**, 2255–2260.
- 78 L. W. Schwartz, H. M. Princen and A. D. Kiss, *J. Fluid Mech.*, 1986, **172**, 259–275.
- 79 F. P. Bretherton, *J. Fluid Mech.*, 1961, **10**, 166–188.
- 80 V. G. Levich, *Physicochemical hydrodynamics*, Prentice-Hall, Englewood Cliffs, 1962.
- 81 F. Brochard, *Langmuir*, 1989, **5**, 432–438.
- 82 F. Sassa, J. Fukuda and H. Suzuki, *Anal. Chem.*, 2008, **80**, 6206–6213.
- 83 K. Choi, A. H. C. Ng, R. Fobel and A. R. Wheeler, *Annu. Rev. Anal. Chem.*, 2012, **5**, 413–440.
- 84 L. Protesescu, S. Yakunin, M. I. Bodnarchuk, F. Krieg, R. Caputo, C. H. Hendon, R. X. Yang, A. Walsh and M. V. Kovalenko, *Nano Lett.*, 2015, **15**, 3692–3696.
- 85 E. M. Chan, *Chem. Soc. Rev.*, 2015, **44**, 1653–1679.
- 86 J. M. R. Narayanam and C. R. J. Stephenson, *Chem. Soc. Rev.*, 2011, **40**, 102–113.
- 87 P. G. Jessop, S. M. Mercer and D. J. Heldebrant, *Energy Environ. Sci.*, 2012, **5**, 7240–7253.
- 88 G. Lestari, A. Salari, M. Abolhasani and E. Kumacheva, *Lab Chip*, 2016, **16**, 2710–2718.

